

Cite this: *Sustainable Food Technol.*,  
2026, 4, 1967

# NADES-based extraction of olive leaf phenolics using RSM, ANFIS and machine learning techniques

Fatiha Brahmi,<sup>\*a</sup> Lokesh Kumar Ramasamy,<sup>b</sup> Selvaraj Kunjiappan,<sup>id c</sup>  
Hayate Guemghar-Haddadi,<sup>a</sup> Kahina Djaoud,<sup>a</sup> Tinhinane Haddad,<sup>a</sup> Hadjer Lamri,<sup>a</sup>  
Lila Boulekbache-Makhlouf<sup>a</sup> and Federica Blando<sup>id \*d</sup>

An environmentally friendly technique was developed for recovering total phenolics (TP) from olive leaves (cv. Chemlal) using a natural deep eutectic solvent (NADES) mixture composed of citric acid/glucose (2 : 1). Optimized extraction parameters were validated through an adaptive neuro-fuzzy inference system (ANFIS) and a random forest regressor machine learning (ML) algorithms. The highest TP yield ( $95.00 \pm 1.49 \text{ mg g}^{-1}$  dry matter, DM) was achieved after 90 min of maceration at 500 rpm with a solid/solvent ratio of 1/70  $\text{g mL}^{-1}$ . Compared with response surface methodology (RSM), a commonly used conventional optimisation approach, the ML-based models displayed greater generalization and prediction accuracy. The extraction process was best optimized by XGBoost and ANFIS, with time and solvent ratio identified as the most influential variables. The optimized extract contained  $0.52 \pm 0.03 \text{ mg g}^{-1}$  DM flavonoids and  $6.64 \pm 0.30 \text{ mg g}^{-1}$  DM tannins, and displayed strong antioxidant activity with  $\text{IC}_{50}$  values of  $194.165 \mu\text{g mL}^{-1}$  (phosphomolybdate),  $3330 \mu\text{g mL}^{-1}$  (DPPH), and  $9750 \mu\text{g mL}^{-1}$  (ABTS). The results demonstrated that the ANFIS model was well aligned with operational data, with a high  $R^2$  of 0.9611, along with the lowest RMSE close to 4.4. Moreover, in this study, ANFIS and ML algorithm models represent a unique contribution beyond NADES/RSM studies. Taken together, these findings highlight the optimal extraction conditions and an eco-friendly solvent mixture never before used for TP recovery from olive leaves, supporting the valorization of olive by-products.

Received 28th October 2025  
Accepted 22nd December 2025

DOI: 10.1039/d5fb00765h

rsc.li/susfoodtech

## Sustainability spotlight

The agri-food sector related to olive growing and olive oil production generates large amounts of olive leaves, an undervalued by-product that contributes to waste accumulation and resource underutilization. With the increase in environmental awareness, there is a growing interest in a circular economy and in the valorization of agro-food by-products, whose value is still underestimated. Addressing this challenge is essential for promoting circular bioeconomy strategies and reducing environmental impacts. This study demonstrated that through an environmentally friendly technique, a high amount of phenolic compounds can be recovered from olive leaves. By valorizing this agro-industrial residue, this study advances sustainable technology for nutraceutical and pharmaceutical sectors, and contributes to resource efficiency, waste reduction, and the development of functional food ingredients. This research aligns with UN sustainable development goals 3 (good health and well-being), 9 (industry, innovation, and infrastructure), and 12 (responsible consumption and production).

## Introduction

The olive plant (*Olea europaea* L.) is one of the oldest cultivated fruit trees in the world and one of the most representative fruit tree species of the Mediterranean basin. Today, nearly 11

million hectares of the plant are cultivated worldwide, predominantly in Greece, Italy, Spain, Australia, Portugal, France, Cyprus, Israel, Jordan, the USA, Morocco, Turkey, and Tunisia.<sup>1</sup>

The olive oil industry represents one of the most prominent agro-industrial sectors in Mediterranean countries, playing a major role in their economic and social development. Over the last 60 years, global olive oil production has tripled. Likewise, olive oil consumption has been increasing not only in the top five producing countries (Spain, Greece, Italy, Turkey, and Morocco) but also in regions outside the traditional cultivation zones.<sup>2</sup>

As an agro-industrial activity, olive oil production has notable environmental impacts, including waste generation.<sup>3</sup> One of the main contributors to this waste is olive leaves, which

<sup>a</sup>University of Bejaia, Faculty of Natural and Life Sciences, Laboratory of Biomathematics, Biochemistry, Biophysics and Scientometry, Bejaia, 06000, Algeria. E-mail: fatiha.brahmi@univ-bejaia.dz

<sup>b</sup>School of Computer Science and Engineering, Vellore Institute of Technology, Vellore, Tamil Nadu, 632014, India

<sup>c</sup>Department of Biotechnology, Sethu Institute of Technology, Kariapatti-626115, Tamil Nadu, India

<sup>d</sup>Institute of Sciences of Food Production (ISPA), National Research Council (CNR), Research Unit of Lecce, Via Prov. le Lecce-Monteroni, 73100 Lecce, Italy. E-mail: federica.blando@cnr.it



are an unavoidable by-product of routine tree pruning and olive harvesting. It is estimated that olive leaves account for approximately 25% of the dry weight of total pruning residues. Olive leaves are also generated as a by-product at olive mills, where they are discarded during the cleaning of olives with a blower machine. They typically account for approximately 10% of the olives' weight.<sup>4</sup>

This large amount of olive leaves adds additional expense for farmers and poses a sustainability challenge, as a significant portion of this by-product remains underexploited, used as a feed additive or inadequately disposed of through incineration or other treatments.<sup>2,5,6</sup>

Historically, olive leaves were generally used in the Mediterranean countries as a medicine to cure fever and other infectious diseases like malaria. In the last decade, the discovery that olive leaves are rich in bioactive compounds with health-promoting properties has attracted increasing interest from researchers worldwide, in line with the growing emphasis on the circular economy in green development.<sup>6–8</sup> Therefore, this waste biomass can provide value-added ingredients for dietary supplements and functional food formulation. Simple phenols, flavonoids, and secoiridoids are the polyphenol classes present in olive leaf extract. In particular, secoiridoids are a characteristic phenolic class in the *Olea* genus.<sup>9</sup> The major secoiridoid compound in olive leaves is oleuropein, which exhibits interesting biological and pharmacological properties, in large part attributed to its putative antioxidant and anti-inflammatory effects.<sup>8,10</sup>

Solid–liquid extraction of phenolic compounds from a plant matrix is typically performed using organic solvents; however, most of these are dangerous and pollute the environment.<sup>11</sup> Green chemistry concepts must be applied across all scientific fields to promote sustainability. Sustainable analytical techniques have been developed based on the principles of green analytical chemistry. Reducing or eliminating the use of by-products and solvents harmful to the environment and human health is currently one of the top concerns.<sup>12</sup> The extraction of natural products, including phenolic compounds, is one of the potential areas where green chemistry principles might have a substantial impact on output quality and productivity.<sup>13</sup>

Recently, natural deep eutectic solvents (NADES) have emerged as alternatives to organic solvents.<sup>14</sup> They are growing in popularity for use in novel sustainable extraction techniques because they are cost-effective, more biodegradable, and less toxic than traditional solvents. Chemical characteristics, including low melting temperatures, low volatility, nonflammability, low vapor pressure, polarity, chemical and thermal stability, and miscibility and solubility, are among the advantages of NADES. Additionally, their low costs and excellent manufacturing yields are linked to a convenient atom economy and a minimal environmental impact. Their formation involves intermolecular hydrogen bonding rather than chemical reactions; therefore, no by-products are formed, eliminating the need for purification and minimizing waste generation.<sup>15</sup>

NADES are a combination of two or three basic components that, when combined at the appropriate molar ratio, have

melting points lower than those of their individual components.<sup>16</sup> These transparent liquid mixtures consist of hydrogen bond donors (HBDs) and acceptors (HBAs). Their components often interact through hydrogen bonding. NADES are regarded as “natural” as the eutectic mixture's constituent parts are primary metabolite groups, including sugars, organic acids and bases, and amino acids. Thus, they can be exploited in food and promote green technologies. Moreover, compared to traditional organic solvents, they effectively generate extracts with greater yields, with broad potential applications including phenolic component recovery from biomass waste.<sup>17,18</sup>

In this study, olive leaves (cv. Chemlal) were extracted using a citric acid and glucose mixture, a NADES combination, which had not previously been used for extracting phenolics from olive leaves.

Complex extraction processes can be modeled and optimized with the help of machine learning (ML) techniques. These methods are able to simultaneously capture non-linear correlations and interactions between several response variables and process parameters.<sup>19,20</sup>

The response surface methodology (RSM) is a statistical technique, which uses a second-order polynomial equation for modeling and optimization. For non-linear systems, to predict the optimal conditions, the adaptive neuro-fuzzy inference system (ANFIS) and machine learning algorithm approaches are also widely used.

Here, RSM was used in conjunction with ML techniques, such as artificial neural networks (ANN), extreme gradient boosting (XGBoost), and ANFIS to improve predictions and optimizations. A central composite design (CCD) was employed to systematically vary and analyze the influence of three key process parameters: extraction time, stirring speed, and solvent-to-solid ratio.

Despite the growing research on NADES and RSM/ML, the specific combination of “olive leaves, NADES, RSM and ML” remains scarcely explored, if not entirely absent from the literature. Moreover, no research papers have investigated the use of RSM and ANFIS to optimize phenolic extraction from olive leaves.

The objective of this study is to maximize the phenolic component recovery for olive leaves (cv. Chemlal) by adopting a new NADES mixture (citric acid and glucose). The study also aims to compare RSM, ANFIS and ML techniques in the optimization process.

## Materials and methods

### Raw material and chemicals

Olive leaves (cv. Chemlal) were harvested in February 2024 from Ahl El Ksar (36°15'11.16" N 4°02'21.98" E, at an altitude of 686 m) southeast of Bouira province (Algeria). The raw material was rinsed three times with tap water and then dried in a ventilated oven (Memmert, Germany) at 40 °C for 48 h. After drying, the leaves were ground into a fine powder ( $\leq 250 \mu\text{m}$ ) using a home grinder and stored at room temperature in paper bags for further analysis.



Analytical grade ethanol (96%), methanol (99%), hydrochloric acid (HCl, 37%), citric acid, and phosphomolybdate ammonium were sourced from Biochem Chemopharma (Cosne-Cours-sur-Loire, France). Gallic acid, catechin, quercetin, vanillin and glucose were purchased from Sigma-Aldrich (St. Louis, MO, USA). Diphenyl-picryl-hydrazyl (DPPH), 2,2'-azino-bis (3-ethylbenzothiazoline-6-sulfonic acid) (ABTS), Folin-Ciocalteu reagent, sodium carbonate anhydrous ( $\text{Na}_2\text{CO}_3$ ) and aluminum chloride ( $\text{AlCl}_3$ ) were purchased from Prolabo (Llinars del Vallès, Spain).

### Preparation of NADES and extracts

To prepare NADES, citric acid was selected as the hydrogen bond acceptor (HBA) and glucose as the hydrogen bond donor (HBD). The HBA (citric acid) and HBD (glucose) were mixed at a 2:1 molar ratio and stirred in a water bath at 50 °C until a clear liquid formed. Additionally, water was added (30% w/w) to increase extraction and reduce viscosity. The material was then allowed to cool at room temperature and stored in sealed containers in a desiccator.<sup>21</sup> The density of the citric acid:glucose mixture was 1748.38  $\text{kg m}^{-3}$  at 20 °C. The dynamic viscosity value for this NADES was around 0.0370 Pa s at 20 °C. Its electrical conductivity increased with temperature in the range of 0.00421–0.03090  $\text{S m}^{-1}$ .<sup>22</sup> A weighed amount of leaf powder was placed in a 100 mL screw-capped conical flask containing the prepared NADES, and stirred at room temperature on a magnetic stirrer (Are Heating Magnetic Stirrer, Velp Scientifica, Usmate (MB), Italy). The time ranged from 30 min to 120 min, and the stirring speed ranged from 100 to 900 rpm. The solvent-to-powder ratio fluctuated from 30/1 to 90/1 ( $\text{mL g}^{-1}$ ). To investigate the optimal process conditions for the NADES extraction, these variables were changed sequentially, while the temperature was kept constant at 25 °C. The powerful solvation ability of NADES allows for effective extraction at room temperature, despite temperature being a critical factor in conventional extractions. To optimize the extraction process based on operational parameters (time, agitation speed, and solvent-to-solid ratio), the temperature was held constant. After the extraction process, the mixture was filtered, and the filtrate was used to measure the total phenol content (TPC).

A schematic diagram summarising the workflow (extraction → analysis → modelling) is shown in Fig. 1.

### Total phenolic content (TPC) measurement

The amount of TPC ( $Y$ ) in the extracts was ascertained by spectrophotometric analysis using the previously mentioned method.<sup>23</sup> In short, 0.5 mL of Folin-Ciocalteu reagent (diluted to 1/10) was combined with 2.5 mL of olive leaf extract. After vortexing the mixture for two minutes, 1 mL of 7.5% sodium carbonate ( $\text{Na}_2\text{CO}_3$ ) was added five minutes later, and the samples were incubated at 50 °C for 15 min. After cooling, the absorbance was measured at 760 nm, using a spectrophotometer (Rayleigh UV-1800, Beijing, China). Gallic acid was used as the reference standard, and the results were expressed as milligrams of gallic acid equivalent (GAE) per gram of dry matter (DM).

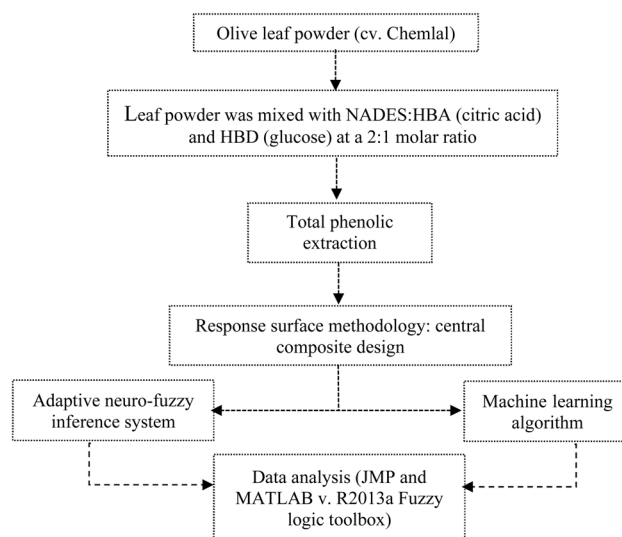


Fig. 1 Schematic workflow diagram illustrating the experimental design for the optimization of phenolic extraction from olive leaves (cv. Chemlal).

### TPC extraction optimization and statistical modelling

**Design and optimization of experiments by RSM.** A three-level, three-factorial central composite design (CCD) was employed. The values of the independent variables, extraction time ( $T$ ), stirring speed ( $S$ ), and solvent-to-solid ratio ( $R$ ), were coded as  $-1$ ,  $0$ , and  $+1$  from low to high (Table 1). Twenty trial runs were carried out using this design. To determine every potential interaction between the input variables and response, the results were fitted to a second-order polynomial model of RSM.

**Adaptive neuro-fuzzy inference system (ANFIS).** This approach uses a rule-based fuzzy logic model that learns using rules created throughout the process. This system uses backpropagation modeling and least squares to give training datasets. The initial phase in training data for the ANFIS is backpropagation of the ANN. Fuzzy logic membership functions are then applied to the ANN's output response as input variables for time ( $T$ ), stirring speed ( $S$ ), and solvent-to-solid ratio ( $R$ ). The optimizations for these variables are more accurate when the fuzzy inference system (FIS) is used. To obtain several inputs ( $T$ ,  $S$ , and  $R$ ) and a single output response ( $Y$ ), the Sugeno-type fuzzy inference model was used for the ANFIS modeling in this study.<sup>19</sup> Multiple inputs and a single output reaction are shown simultaneously in the ANFIS architecture (Fig. 2).

Table 1 Levels of factors chosen for the extraction experiments

Independent variables	Factor levels		
	$-1$	$0$	$+1$
$T$ (time, min)	60	90	120
$S$ (stirring speed, rpm)	100	300	500
$R$ (solid-to-liquid ratio, $\text{g mL}^{-1}$ )	1/70	1/80	1/90



A FIS has two inputs, “x” and “y,” and one output response, “z.” The following is an expression for two fuzzy if-then rules for a first-order Sugeno fuzzy model:

Rule 1:  $f_1 = p_1x + q_1y + r_1$  if  $x$  is  $A_1$  and  $y$  is  $B_1$ . Rule 2:  $f_2 = p_2x + q_2y + r_2$  if  $x$  is  $A_2$  and  $y$  is  $B_2$ , where  $A_1$  and  $B_1$  are the fuzzy sets,  $f_1$  is the output response, and  $p_1$ ,  $q_1$ , and  $r_1$  are the design parameters, which were established during the training phase.

Trial and error were used to establish the number of membership functions for each input variable.

**Machine learning algorithm.** A random forest regressor was applied, as the target values of the experiment were continuous. This ensemble method constructs multiple decision trees, each trained on a randomly selected subset of features and training data, which reduces overfitting and improves predictive performance. The final prediction is obtained by aggregating the outputs of all decision trees, resulting in a more robust and accurate model.<sup>19</sup>

In this study, the experimental variables  $T$ ,  $S$ , and  $R$  were used as inputs, while  $Y$  served as the output response. The dataset was first imported for prediction and then pre-processed to identify and handle noisy or missing data.

### Total flavonoid and condensed tannin content (TFC) of the optimized extract

The procedure reported by Brahmi *et al.* (2022)<sup>24</sup> was used to calculate the TFC of the optimized extract. 1 mL of 2% aluminum chloride solution was combined with 1 mL of the sample extract. After 15 min of incubation in a dark environment, the absorbance was measured at 430 nm. The results were displayed in milligrams of quercetin equivalent (QE) per gram of material (mg QE/g DM).

To determine the amount of condensed tannins, the procedure already reported was followed.<sup>25</sup> The extract (50  $\mu$ L) and 4% vanillin/methanol solution (150  $\mu$ L) were combined, and the resulting mixture was vortexed. After incubation for 24 h at 4 °C, 750  $\mu$ L of HCl was added; then, the solution was allowed to sit at room temperature for 20 min. The absorbance was measured at 550 nm, and the concentration was expressed as milligrams of tannic acid equivalent per gram of dry matter (mg TA/g DM).<sup>26</sup>

### Evaluation of the antioxidant properties of the optimized extract

For the antioxidant activity, 200  $\mu$ L of optimized extract and two mL of ammonium phosphomolybdate reagent [ $\text{H}_2\text{SO}_4$  (0.6 M),  $\text{Na}_2\text{HPO}_4$  (28 mM) and ammonium phosphomolybdate (4 mM)] were added, and the mixture was incubated at 90 °C for 90 min in a water bath. The absorbance was read at 695 nm, after cooling.<sup>24</sup>

For the assessment of the antioxidant capacity using the DPPH scavenging test, two mL of extract were combined with 150  $\mu$ L of DPPH free radical solution (0.1 mM DPPH in ethanol); the mixture was then incubated for 60 min at ambient temperature.

The absorbance was measured at 517 nm and using eqn (1), the percentage of DPPH radical scavenging capacity was determined.<sup>27</sup>

The ABTS free radical scavenging potential was calculated in accordance with our previous study.<sup>27</sup> Briefly, 7 mM ABTS radical solution was combined with 2.45 mM potassium persulfate, and the resulting reaction mixture was left at room temperature for 16 h in the dark. The absorbance of the reaction mixture was then adjusted to  $0.70 \pm 0.05$  at 734 nm using ethanol. 10  $\mu$ L of optimized extract was combined with 1 mL of this reaction mixture. The following equation was used to calculate the inhibitory activity:

$$\text{Inhibition \%} = \frac{[\text{absorbance}_{\text{control}} - \text{absorbance}_{\text{sample}}]}{\text{absorbance}_{\text{control}}} \times 100 \quad (1)$$

All results were expressed as  $\text{IC}_{50}$  (mg mL<sup>-1</sup>).

### Statistical analysis

Every assay was carried out three times to calculate mean values and standard deviations. The ANOVA test was performed to compare the means, and significant differences were considered at a  $p$ -value of 0.05.

CCD trials were carried out and JMP.7 regression was used to analyze the experimental results. The experimental data were separated for training, testing, and validation of the network model using MATLAB v. R2013a fuzzy logic toolbox to forecast the results of the extraction of a significant amount of phenolics from olive leaves.

## Results and discussion

### Usage of RSM to analyze experimental results

In this investigation, the modeling and prediction of phenolics from olive leaves (cv. Chemlal) extracted by NADES were performed.

Only recently, phenolics from olive leaves have been extracted using various combinations of NADES.<sup>28–42</sup> Table 2 reports previous studies in the literature on the use of NADES for extracting phenolics from olive leaves.

In the present study, a new mixture of NADES (citric acid and glucose) was utilized. To the best of our knowledge, this combination has not yet been applied for the extraction of

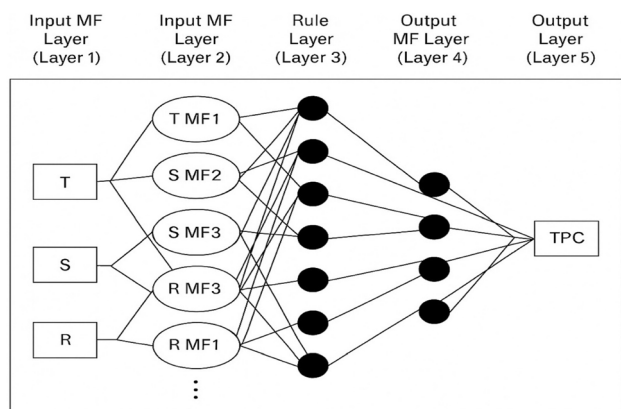


Fig. 2 Adaptive neuro-fuzzy inference system (ANFIS) architecture for olive leaf extraction model precision. T: time, S: speed, R: ratio, MF: membership function, TPC: total phenolic content.



Table 2 Previous studies in the literature on the use of NADES for extracting phenolics from olive leaves<sup>a</sup>

Variety and origin	Extraction method	Optimal NADES used	TPC	Reference
Hojiblanca Seville (Spain)	Microwave-assisted extraction-RSM	Choline chloride-ethylene glycol (1 : 2)	28.52 mg g <sup>-1</sup>	28 (Alañón <i>et al.</i> , 2020)
Agrielia Kalamon	Batch stirred-tank extraction/RSM	Glycine : L-lactic acid (1 : 5)	96.41 mg g <sup>-1</sup>	29 (Kaltisa <i>et al.</i> , 2020)
Avlida (Evia, central Greece)	Batch stirred-tank polyphenol extraction/RSM	L-lactic acid and ammonium acetate at 7 : 1 with $\beta$ -cyclodextrin	113.66 mg g <sup>-1</sup>	30 (Chakroun <i>et al.</i> , 2021)
Koroneiki Chania (Greece)	Conventional heating extraction/RSM	Choline chloride with acetic acid	325.12 mg kg <sup>-1</sup>	31 (de Almeida Pontes <i>et al.</i> , 2021)
Camanducaia (Brazil)	Ultrasound-assisted extraction-RSM	Choline chloride-fructose-water (5 : 2 : 5)	187.31 $\pm$ 10.3 mg g <sup>-1</sup>	32 (Ünlü, 2021)
No cv. Burhaniye, Balıkesir (Turkey)	Microwave-assisted extraction	Choline chloride : acetic acid (1 : 2) and ethanol (80 : 20 w/w)	4438 $\pm$ 89 mg L <sup>-1</sup>	33 (Boli <i>et al.</i> , 2022)
Messinia (Greece)	Batch extraction-RSM	Glycerol : lysine (3 : 1)	188.39 $\pm$ 0.37 mg g <sup>-1</sup>	34 (Akli <i>et al.</i> , 2022)
Koroneiki Chania (Greece)	Magnetic stirring in an oil bath/RSM	Glycerol, citric acid, and L-proline (2 : 1 : 1)	42.48 mg g <sup>-1</sup>	35 (Athanasiadis <i>et al.</i> , 2022)
Agrielia Kalamon Evia (Greece)	Continuous stirring/RSM	Glycerol/citric acid 4 : 1	69.35 mg g <sup>-1</sup>	36 (Houasni <i>et al.</i> , 2022)
Koroneiki (Greece)	Sonication by a probe inside the water bath: ANN	Choline chloride : L,2-propanediol : levulinic acid (1 : 1 : 1) with 20% water	Rutin and flavones: 46.4 mg g <sup>-1</sup>	37 (Alrugaibah <i>et al.</i> , 2023)
Arbosana Florida (USA)	Microwave, ultrasound, homogenate and high hydrostatic pressure	Choline chloride with citric acid 1 : 2	55.12 $\pm$ 1.08 mg g <sup>-1</sup>	38 (Siamandoura and Tzia, 2023)
Argentina Thiva, Viotia (Greece)	Stirring in a water bath	Choline chloride : glycerol (1 : 5 ratio with 30% water)	n.d.	39 and 40 (Mir-Cerdà <i>et al.</i> , 2023 and 2024)
Arbequina, Verdiella Huesca (Spain)	Solid-liquid extraction with mechanical stirring and microwave-assisted extraction	Choline chloride with glycerol, lactic acid and ethylene glycol	20 mg g <sup>-1</sup>	41 (Tapia-Quirós <i>et al.</i> , 2025)
Arbequina, Verdiella Huesca (Spain)	Mechano-chemical extraction/RSM	Choline chloride : glycerol (3 : 1)	1.3 $\pm$ 0.3 mg g <sup>-1</sup>	42 (Cubero-Cardoso <i>et al.</i> , 2025)

<sup>a</sup> dm: dry matter, dw: dry weight, n.d.: not determined, TPC: total phenolic content.

phenolic compounds from olive leaves. In particular, this NADES mixture was chosen to evaluate the extraction conditions, in terms of the general and global output, for the total phenolic content (evaluated by the widely used Folin–Ciocalteu assay) and antioxidant capacity (evaluated by three distinct assays, as recommended). We were not interested in studying the selective extraction of specific phenolic compounds from olive leaves, which will be addressed in a future study.

Several methods for maximizing polyphenol extraction from olive leaves using NADES have been reported, including ultrasound-assisted extraction,<sup>32</sup> microwave-assisted extraction,<sup>33</sup> and solid–liquid extraction with stirring,<sup>29,31,34,39,40</sup> all of them with or without temperature control. NADES demonstrated superior extraction performance compared to conventional solvents, including ethanol.<sup>30–39</sup>

We chose to use a new mixture, highly sustainable in terms of cost, food compatibility, and safety.

From a mechanistic point of view of the solvent–solute interaction, it can be assumed that the quantity and distribution of hydroxyl groups, the acceptor-to-donor molecular ratio, or the structure of the hydrogen bond donor are important factors influencing the solubility of phenolic compounds in NADES. Their structure allows for the accommodation of many phenolic molecules *via* interactions with aliphatic protons. High solubility of phenolic compounds occurs when hydroxyl groups are present in their structure.<sup>43</sup> Citric acid and glucose contain numerous hydroxyl groups (–OH) capable of forming hydrogen bonds with polyphenolic compounds such as oleuropein and hydroxytyrosol. These interactions promote the association of polyphenols with the NADES, increasing their solubility and, consequently, enhancing the amount of polyphenolic compounds that can be extracted.

Furthermore, the strong polarity of the glucose–citric acid combination enhances the solubility of naturally polar polyphenolic compounds. This high polarity improves the extraction efficiency by facilitating the disruption of interactions between polyphenols and the plant matrix. In addition, the acidic environment provided by citric acid contributes to the stabilization of polyphenols during extraction. By limiting oxidation and degradation processes, an acidic pH helps preserve the integrity and purity of the extracted compounds.<sup>44</sup>

To assess the effect of variables on the NADES extraction process, a CCD–RSM optimisation was created using the coded parameters *T* (time), *S* (speed), and *R* (ratio) (Table 3). The experimental design was established on the basis of the coded level of the aforementioned three variables, resulting in 20 experimental runs with six replicates of the central point.

The model has a better agreement with the input parameters, as indicated by its coefficient of determination ( $R^2$ ) of 0.9495. Similarly, the findings of the error analysis showed a negligible lack of fit ( $p > 0.05$ ) of 2.4113 (Table 4).

The generated model is reproducible, as evidenced by the coefficient of variation (C.V.) of 3.88, which is less than 5%. The model's relevance is implied by its higher F value of 20.88 with a correction coefficient (adj  $R^2$ ) of 0.9040. This fits the practical test and explains 90.40% of the change in the response value.

After deleting the non-significant variables, the following mathematical equation (eqn (2)) shows the relationship between the three independent factors and the TPC response (*Y*) of olive leaves:

$$Y = 72.99 - 1.98T + 5.53S + 3.10R + 5.46TS + 3.43TR + 3.78SR - 10.95TT + 3.51SS + 13.60RR \quad (2)$$

**Table 3** CCD matrix of three independent variables applied to the extraction of 'Chemlal' olive leaves by NADES, and the resulting total phenolic contents (TPC)

Run no.	<i>T</i> (min)	<i>S</i> (rpm)	<i>R</i> (mL g <sup>-1</sup> )	TPC (mg GAE per g DM)			
				Experimental	RSM	ANFIS	ML algorithm
1	90	300	70	85.05	83.48	84.67	84.92
2	120	500	90	92.36	90.92	91.27	101.57
3	90	300	80	70.74	72.99	74.51	89.33
4	90	100	80	68.21	70.96	70.29	67.45
5	90	300	80	73.92	72.99	73.58	74.18
6	120	500	70	82.01	85.41	84.67	83.24
7	60	500	90	74.98	77.08	75.12	65.31
8	90	300	80	74.51	72.99	72.51	65.87
9	120	100	90	75.25	76.49	75.81	74.92
10	120	100	70	57.94	55.86	57.13	58.67
11	90	300	90	88.22	89.69	88.91	87.45
12	60	500	70	86.51	85.3	85.15	85.93
13	90	300	80	69.59	72.99	72.56	68.12
14	60	100	90	87.88	84.51	86.43	86.24
15	90	300	80	73.70	72.99	72.07	54.89
16	90	500	80	84.88	82.03	83.21	83.76
17	60	300	80	62.99	64.02	64.59	71.45
18	90	300	80	75.28	72.99	72.01	66.01
19	60	100	70	76.14	77.6	77.23	65.33
20	120	300	80	61.18	60.06	59.84	59.12



Table 4 Analysis of variance for the selected dependent variables

Source	Sum of squares	df	Mean square	F value	p-value, prob > F
Model	1636.68	9	181.85	20.88	<0.0001
Extraction time ( <i>T</i> )	39.05	1	39.05	4.48	0.0603
Stirring speed ( <i>S</i> )	306.03	1	306.03	35.13	0.0001
Ratio ( <i>R</i> )	96.35	1	96.35	11.06	0.0077
<i>T</i> × <i>S</i>	238.82	1	238.82	27.42	0.0004
<i>T</i> × <i>R</i>	94.19	1	94.19	10.81	0.0082
<i>S</i> × <i>R</i>	114.23	1	114.23	13.11	0.0047
<i>T</i> <sup>2</sup>	329.81	1	329.81	37.86	0.0001
<i>S</i> <sup>2</sup>	33.85	1	33.85	3.89	0.0770
<i>R</i> <sup>2</sup>	508.54	1	508.54	58.38	<0.0001
Residual	87.10	10	8.71		
Lack of fit	61.55	5	12.31	2.4113	0.1784
Pure error	25.55	5	5.11		
Cor total	1723.79	19			
<i>R</i> <sup>2</sup>	0.9495				
<i>R</i> <sup>2</sup> adj	0.9040				
<i>R</i> <sup>2</sup> pred	0.4026				
C.V. %	3.88				

Significant effects are seen for the ratio ( $p = 0.0077$ ), and stirring speed ( $p = 0.0001$ ). Additionally, the time × stirring speed, time × ratio, and stirring speed × ratio all exhibited significant interactions with one another, indicating a relationship between their effects.

The squared effect of time ( $p = 0.0001$ ) suggests that the relationship between time and the dependent variable is non-linear. Likewise, a non-linear link between the ratio and the dependent variable is indicated by the squared effect of the ratio ( $p < 0.0001$ ). However, there appears to be a linear relationship between stirring speed and the dependent variable, as evidenced by the non-significant interaction between stirring speed and itself ( $p = 0.0770$ ).

Another way to depict the regression equation is as a three-dimensional response surface (Fig. 3). The relationship between the stirring speed and the solid-to-liquid ratio is shown in Fig. 3a, and an increase in the ratio had a detrimental influence on the TPC yield. According to the relationship between the ratio and extraction time (Fig. 3b), a low ratio and extraction time both constrain the amount of TPC. The relationship between speed and extraction time is depicted in Fig. 3c, and it positively affects the amount of TPC. By maximizing the desirability, the mathematical formula made it possible to determine the ideal circumstances for TPC recovery from olive leaves, which included a ratio of 1/70 ( $\text{g mL}^{-1}$ ), a stirring speed of 500 rpm, and a time of 90 min.

Experiments were repeated using these inferred processing settings to compare the practical value with the predicted value (96.30 mg GAE per g DM). The real study yielded a mean value of  $95.00 \pm 1.49$  mg GAE per g DM ( $n = 3$ ), demonstrating the model's efficacy as there were no significant differences between the actual and the predicted values for TPC ( $p > 0.05$ ).

#### Modeling with an adaptive neuro-fuzzy inference system (ANFIS)

The main benefit of ANFIS over artificial neural networks (ANN) is that it blends fuzzy logic and neural network best practices to more

precisely and accurately describe complex systems.<sup>19</sup> In order to forecast the extraction variables of olive leaf extracts along with validating experimental data, ANFIS modeling was employed. To create the ANFIS model prediction, the same 20 experimental data sets that are displayed in Table 3 were split into three sets for training and testing data sets and model validation. Then, these sets were utilized to build a fuzzy inference system, whose parameters were modified for the membership function using the backpropagation technique and the least-squares approach. A FIS of ANFIS model with membership functions, one output response, and three input responses needs to be built in order to guarantee accuracy. As shown in Fig. 2, the suggested design of the ANFIS model consists of one output value and five input variables. One by one, a number of parameters need to be checked. There are three fuzzy sets: low, medium, and high for each of the input variables, such as extraction time (*T*), speed (*S*), and ratio (*R*).

Similarly, the TPC ( $91.00 \pm 1.49$  mg GAE per g) was specified in five fuzzy sets—very low, low, medium, high, and very high—based on experimental results for the expected output response. The fuzzy rule was constructed using data from human observations and experiments. RSM was utilized to improve the fuzzy rules using the projected values of the response.

#### Modeling with the ML algorithm

The use of ML to optimize phenolic compound extraction from olive leaves is currently mainly unexplored, despite its potential. Only Rodríguez-Fernández *et al.* (2023)<sup>45</sup> modelled phenolic extraction from leaves of a Turkish olive cultivar using ultrasound-assisted extraction optimized by machine learning.

The experimental parameters, namely extraction time (*T*), speed (*S*), and ratio (*R*), are selected as inputs, and TPC (*Y*) is the output data. The random forest regressor model was developed by changing the model's output data while maintaining constant input data because the dataset includes the five target columns. *R*<sup>2</sup> score error computation is used to evaluate the models after they have been fitted to the training set of data.



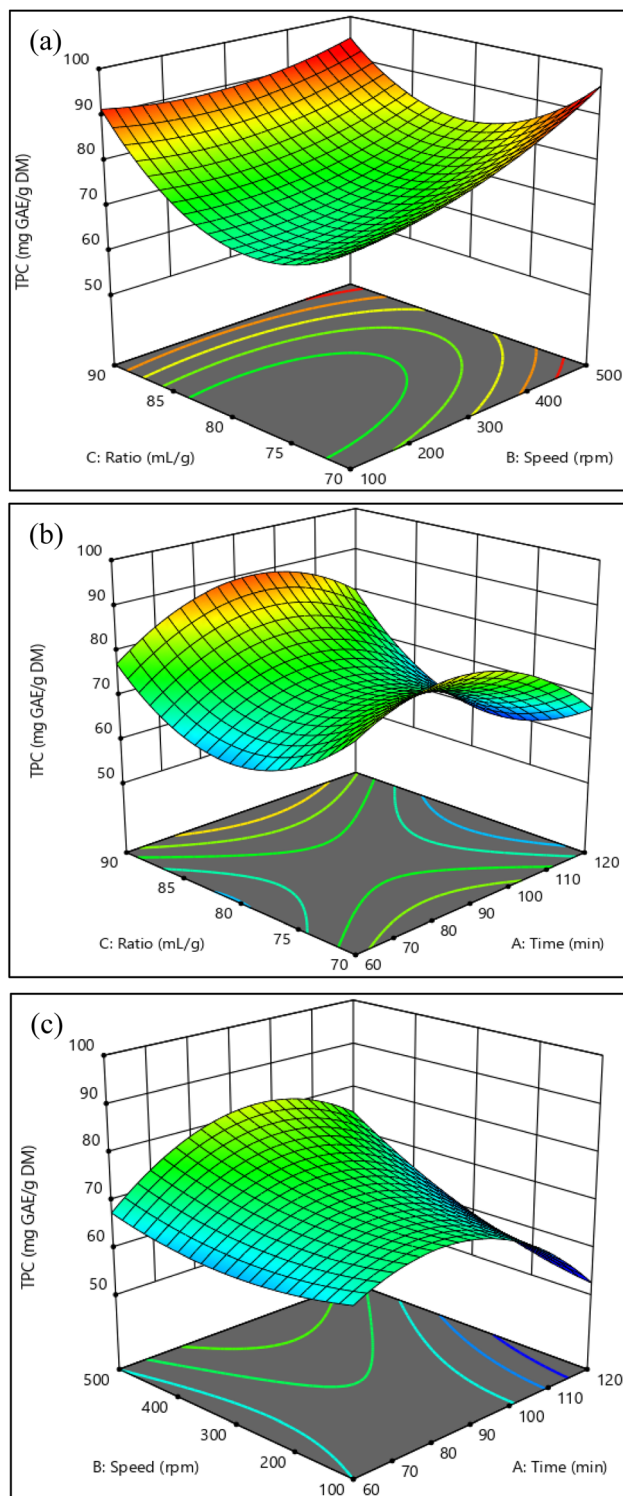


Fig. 3 Response surface methodology (RSM) graphical analysis. (a–c) Demonstrations of the effect of time, speed, and solid-to-liquid ratio on the total phenolic content of 'Chemlal' olive leaves.

The model then predicts the input values ( $T$ : 90 min,  $S$ : 500 rpm,  $R$ : 70 mL g<sup>-1</sup>). The expected output response for TPC (101.57 mg GAE per g) was reached based on the experimental results. To illustrate the error variation between the actual and anticipated values, a graph model (Fig. 4) was created.

### Model validation

The optimized extraction parameters for the TPC were validated using the RSM results. The validation experiments were conducted using Design Expert software, which could determine the best extraction settings and their combinations. For the same data, the ANFIS and machine learning algorithm models were employed, and the optimum conditions were also confirmed.

A rule viewer plot (Fig. 5) was used to observe the values of the responses upon varying the process variables. The rule viewer is a condensed toolset that has fuzzification and neural weight optimization built in. Here, the rule viewer plot tool was used to anticipate the response variables for different model inputs. Further cross-validation of the model was made possible by conducting tests and comparing the results with the predicted values of the model.

At the desired optimal settings for the extraction parameters ( $T$  = 90 min,  $S$  = 500 rpm,  $R$  = 70 mL g<sup>-1</sup>), the expected response for the extract of olive leaves, as determined by the ANFIS model, was 91.27 mg GAE per g. The value for TPC was 101.57 mg GAE per g for the machine learning algorithm model. The results showed that the experimentally measured values and the predictions from RSM, ANFIS, and machine learning modeling fit each other well.

### Comparative study of the different models

Twenty experimental runs were conducted, and the TPC values obtained served as the basis for training and evaluating the performance of multiple models. Model performance was evaluated using the coefficient of determination ( $R^2$ ) and root mean square error (RMSE) calculated for the test dataset.

The RSM model, developed using a second-order polynomial, provided a good approximation of the TPC trends with an RMSE of approximately 7.2, but was limited in capturing highly non-linear relationships.

The ANN model, built using a multilayer perceptron with backpropagation, slightly improved prediction quality, especially where interactions were non-linear. However, XGBoost demonstrated superior performance with an RMSE of around 4.8, owing to its boosting mechanism and ability to model complex variable dependencies.

The ANFIS model showed the best predictive accuracy ( $R^2$  = 0.9611), followed by considerably lower performance from the ML model ( $R^2$  = 0.2802).

Compared to RSM, the ML model showed a greater divergence. This is explained by the fact that ML is a data-intensive non-linear learning technique that needs a sizable training dataset in order to achieve robust generalization. Because our experimental matrix was relatively small and tuned for RSM, ML tended to overfit the training data, which resulted in larger prediction errors. This explains why RSM has better predictive performance and is more reliable when dealing with small, structured experimental designs.

Among all models, ANFIS stood out due to its hybrid architecture combining fuzzy logic and neural networks. It utilized three membership functions per input variable, forming a rule



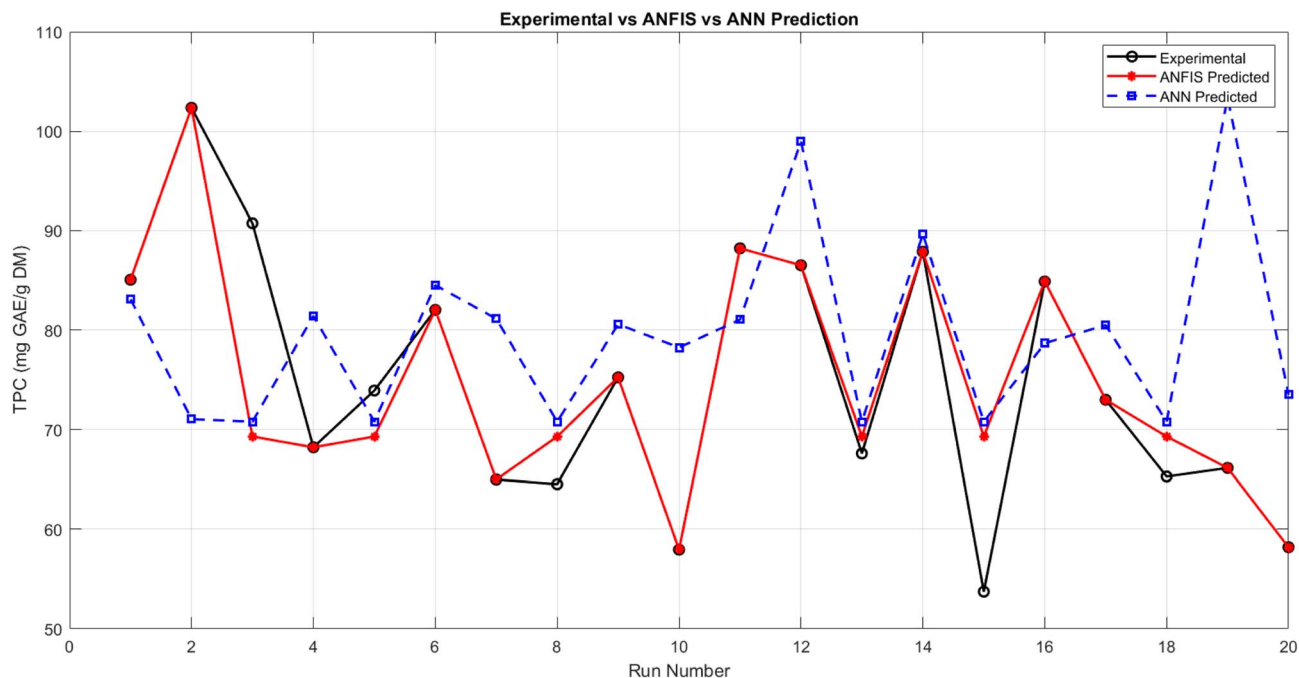


Fig. 4 The validation by the adaptive neuro-fuzzy inference system (ANFIS) and artificial neural network (ANN) of the experimental and predicted results.

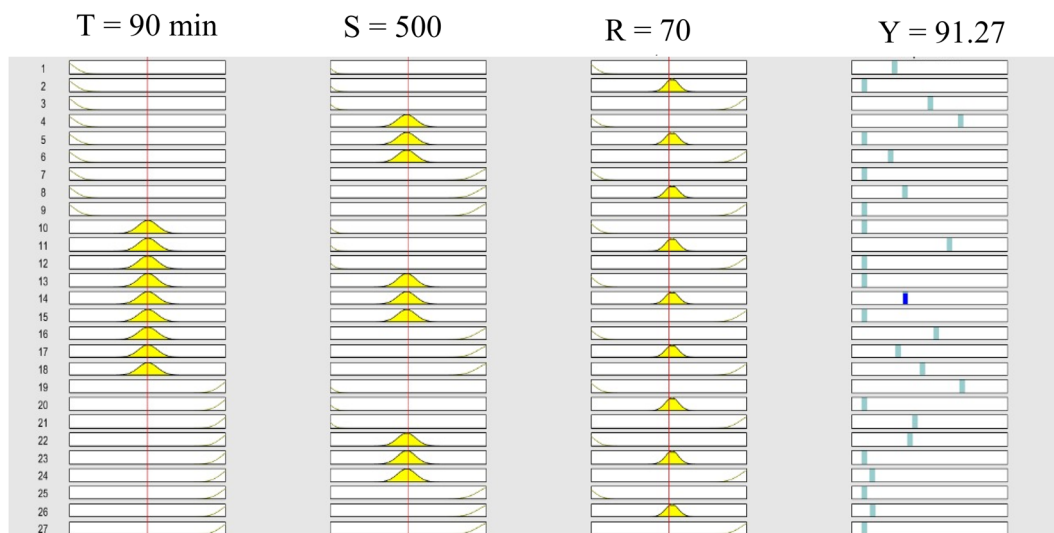


Fig. 5 Adaptive neuro-fuzzy inference system (ANFIS) rule viewer for the effect of extraction parameters on responses for the extraction of total phenolics from 'Chemlal' olive leaves.

base of 27 fuzzy rules, and achieved an RMSE close to 4.4. The ANFIS structure was visualized in MATLAB, showing five layers including input, membership functions, rule base, output membership functions, and final output node. These results clearly show that ANFIS outperforms ML in modelling the non-linear extraction system with a small dataset.

#### Phenolic contents of the optimized extract

Using the extraction conditions already tested in other studies<sup>29,31,34,39</sup> the extract of olive leaves of the cv. Chemlal

exhibited an increased polyphenol content, which ranged from 57.94 to 92.36, with a mean value of 76.07 mg GAE per g DM (Table 2). The average TPC value was higher or similar to the results reported in the above-mentioned studies, using NADES with stirring plus temperature.

After the optimization studies, the optimized extract exhibits a considerable amount of total phenolics ( $95.00 \pm 1.49$  mg GAE per g DM) (Table 5).

Under physical conditions similar to those we used, choline chloride (ChCl) combined with glycerol, at 80 °C for 2 h, was



**Table 5** Phenolic content and antioxidant capacity of the optimized extract from olive leaves (cv. Chemlal)

Assay	Result
<b>Phenolic content (mg per g dry matter)</b>	
Total phenolic content	95.00 ± 1.49
Total flavonoid content	0.52 ± 0.03
Total tannin content	6.64 ± 0.33
<b>Antioxidant capacity (IC<sub>50</sub> μg mL<sup>-1</sup>)</b>	
Phosphomolybdate	159.01 ± 9.02
DPPH radical scavenging capacity	1357.00 ± 21.21
ABTS radical scavenging capacity	7200.00 ± 14.14

able to extract most polyphenols, although the authors did not report a TPC as a Folin–Ciocalteu assay.<sup>39</sup>

ChCl and acetic acid were the best combination to extract most polyphenols from olive leaves, with stirring plus temperature, giving a maximum of 34 mg GAE per g DW.<sup>31</sup>

When using NADES solvents (glycerol with three amino acids: lysine, proline, and arginine), a range of TPC values was obtained (from 67.40 to 177.54 mg GAE per g DM).<sup>34</sup>

Our findings are also comparable to those of Kaltsa *et al.* (2020),<sup>29</sup> who studied the Agrielia Kalamon variety of olive leaves employing NADES, made up of glycine and L-lactic acid. A liquid-to-solid ratio of 36 mL g<sup>-1</sup> and a stirring speed of 500 rpm were the optimal process variable settings with an overall polyphenol yield of 97.53 mg GAE per g DM.

Nonetheless, the measured TPC in our system was lower than those reported by Unlü *et al.* (2021),<sup>32</sup> who reported a maximum level of 187.31 ± 10.30 mg GAE per g DM at the optimized conditions, with choline chloride–fructose–water. In that case, the author used an ultrasound-assisted extraction. Higher TPC values were achieved by Chakroun and co-authors (2021)<sup>30</sup> using β-cyclodextrin and L-lactic acid/ammonium acetate for olive leaves of the Greek cv. Koroneiki. Using ideal extraction parameters (300 rpm stirring speed, a liquid–solid ratio of 100 mL g<sup>-1</sup>, at 80 °C), a TPC result of 113 mg caffeic acid equivalents per g DM was obtained.

As for total flavonoids, with a concentration of 0.52 ± 0.03 mg EQ per g DM, the extract contains a low amount. This value does not reflect what other authors have found.<sup>29,32</sup> It is well known that the main compounds present in olive leaves are oleuropein, hydroxytyrosol and luteolin 7-glucoside. It can be assumed that the combination of citric acid and glucose used here as a NADES can extract a small amount of flavonoids (luteoline 7-glu) relative to secoiridoids.

Tannins may be found in substantial quantities in olive leaves. In our extract, an amount of 6.64 ± 0.30 mg EC per g DM was measured. The values reported in previous studies are lower<sup>46,47</sup> or higher<sup>48</sup> than this amount. These variations may be attributed to the different methodological procedures used for phytochemical analysis.

Moreover, a number of variables, including climate, soil composition, date of collection, drying conditions, cultivation zone, and cultivar, can affect the qualitative and quantitative phenolic composition of olive leaves.<sup>4</sup> Together with these

factors of variability, there are also the consequences of the processing methods and the storage conditions before extraction.<sup>49</sup>

### Antioxidant activity of the optimized extract

According to all assays, remarkable antioxidant capacity was demonstrated by the ‘Chemlal’ olive leaf optimized extract (Table 5). The total antioxidant activity, which evaluates the ability to reduce molybdate ions, demonstrated a better performance with a significant difference ( $p \leq 0.05$ ) with an IC<sub>50</sub> value of 159.01 ± 9.02 μg mL<sup>-1</sup>. Additionally, the leaves extract exhibited a significant ability to neutralize DPPH and ABTS radicals, with corresponding IC<sub>50s</sub> of 1357.00 ± 21.21 and 7200.00 ± 14.14 μg mL<sup>-1</sup>.

The abundance of phenolics, particularly oleuropein, in the leaf extract contributes to these effects, as it is well known that the TPC is highly correlated with the antioxidant leaf extract exhibiting a significant ability to neutralize DPPH and ABTS radical activity.<sup>50</sup>

In the literature, the DPPH test is more suited for assessing olive leaf antioxidant capacity. Still, the results are not of the same magnitude or presented in the same manner as those in this study. In the DPPH assay, various olive leaf extracts from Greece exhibited a powerful anti-DPPH capacity with IC<sub>50</sub> varying from 30.2 ± 3.8 to 126.3 ± 9.5 μg mL<sup>-1</sup>.<sup>51</sup> The results of the same test demonstrated significant antiradical activity of ‘Chemlal’ and ‘Sigoise’ ethanolic extracts with IC<sub>50</sub> values ranging from 98.94 ± 1.01 μg mL<sup>-1</sup> to 188.85 ± 3.65 μg mL<sup>-1</sup>.<sup>49</sup>

## Conclusions

The current investigation attempts to optimize the NADES-based extraction of phenolic compounds from ‘Chemlal’ olive leaves using RSM. The results were compared and validated using ANFIS modeling with an ML algorithm.

The RSM predicted result for the olive leaf extract was 96.30 mg GAE per g at the intended optimal extraction parameter settings ( $T = 90$  min,  $S = 500$  rpm,  $R = 70$  mL g<sup>-1</sup>). According to the ANFIS model, the predicted response was 91.27 mg GAE per g. At the moment when the machine learning algorithm model predicted the reaction, the TPC value was 101.57 mg GAE per g. The findings demonstrated a good fit between the predictions from RSM, ANFIS, and machine learning modeling and the experimentally measured value (95.00 mg GAE per g).

The comparative results demonstrated that ML-based models provided higher prediction accuracy and better generalization compared to traditional RSM. The XGBoost and ANFIS models were particularly effective in optimizing the extraction process, with time and solvent ratio identified as the most influential parameters. This comprehensive modeling framework provides a robust approach for enhancing phenolic compound extraction from olive leaves, offering valuable insights for industrial applications in the nutraceutical and pharmaceutical sectors, with industrial relevance.

Furthermore, the NADES employed (citric acid and glucose), besides being safe for both operators and food-related



applications, appears to exhibit greater selectivity towards secoiridoids (oleuropein) than flavonoids (luteolin) present in olive leaves. Future investigations will be directed at confirming this hypothesis.

## Author contributions

Conceptualization, F. BR.; methodology, T. H and H. I.; software, L. K. R., S. K and H. G-H.; validation, F. BR. and F. BL.; formal analysis, F. BR.; investigation, F. BR. and S. S; resources, A. O. and F. BR.; data curation, F. BR., A. O., and Y. A.; writing—original draft preparation, F.BR.; writing—review and editing, F. BR, F. BL. and K. D; visualization, F. BR.; supervision, L. B-M.; project administration, L. B-M. and H. G-H. All authors have read and agreed to the published version of the manuscript.

## Conflicts of interest

There are no conflicts to declare.

## Data availability

Data are available upon request from the authors, as raw data associated with laboratory notebooks and Excel data sheets.

## Acknowledgements

We gratefully acknowledge the financial support provided by the Direction Générale de la Recherche Scientifique et du Développement Technologique (DGRSDT) as part of the PRIMA 2023-FoWRSaP project.

## References

- <http://faostat.fao.org/site/567/DesktopDefault.aspx?PageID=567#anchor>, (accessed July 1 2025).
- J. Espeso, A. Isaza, J. Y. Lee, P. M. Sørensen, P. Jurado, R. d. J. Avena-Bustillos, M. Olaizola and J. C. Arboleya, *Front. Sustainable Food Syst.*, 2021, 5, 660582.
- G. Enaime and M. Lübken, *Appl. Sci.*, 2021, 11, 8914.
- L. Abaza, A. Taamalli, H. Nsir and M. Zarrouk, *Antioxidants*, 2015, 4, 682–698.
- N. Rahmanian, S. M. Jafari and T. A. Wani, *Trends Food Sci. Technol.*, 2015, 42, 150–172.
- F. S. Markhali, J. A. Teixeira and C. M. Rocha, *Processes*, 2020, 8, 1177.
- C. D. Goldsmith, Q. V. Vuong, C. E. Stathopoulos, P. D. Roach and C. J. Scarlett, *Antioxidants*, 2014, 3, 700–712.
- M. M. Özcan and B. Matthäus, *Eur. Food Res. Technol.*, 2017, 243, 89–99.
- D. Boskou, in *Olive and Olive Oil Bioactive Constituents*, Elsevier, 2015, pp. 1–30.
- O. Benavente-Garcia, J. Castillo, J. Lorente, A. Ortuño and J. Del Rio, *Food Chem.*, 2000, 68, 457–462.
- D. R. Joshi and N. Adhikari, *J. Pharm. Res. Int.*, 2019, 28, 1–18.
- S. S. Ferreira, T. A. Brito, A. P. Santana, T. G. Guimarães, R. S. Lamarca, K. C. Ferreira, *et al.*, *Talanta Open*, 2022, 6, 100131.
- A. Ali Redha, *J. Agric. Food Chem.*, 2021, 69, 878–912.
- Y. Dai, J. Van Spronsen, G.-J. Witkamp, R. Verpoorte and Y. H. Choi, *Anal. Chim. Acta*, 2013, 766, 61–68.
- C. Canavacciolo, S. Pagliari, J. Frigerio, C. M. Giustra, M. Labra and L. Campone, *Foods*, 2022, 12(1), 56.
- E. Chev e-Kools, Y. H. Choi, C. Roullier, G. Ruprich-Robert, R. Grougnet, F. Chapeland-Leclerc and F. Hollmann, *Green Chem.*, 2025, 27, 8360–8385.
- N. P. E. Hikmawanti, D. Ramadan, I. Jantan and A. Mun'im, *Plants*, 2021, 10(10), 2091.
- Y. Liu, J. B. Friesen, J. B. McAlpine, D. C. Lankin, S.-N. Chen and G. F. Pauli, *J. Nat. Prod.*, 2018, 81, 679–690.
- S. Kunjiappan, L. K. Ramasamy, S. Kannan, P. Pavada, P. Theivendren and P. Palanisamy, *Sci. Rep.*, 2024, 14, 1219.
- I. Bouaziz, M. Hentabli, M. K. Amar, M. Laidi, A. Bouzidi, H. Bouzemlal, *et al.*, *J. Supercrit. Fluids*, 2026, 227, 106755.
- L. Meneses, F. Santos, A. R. Gameiro, A. Paiva and A. R. C. Duarte, *J. Visualized Exp.*, 2019, 152, e60326.
- D. Z. Troter, M. Z. Zlatković, D. R. Đokić-Stojanović, S. S. Konstantinović and Z. B. Todorović, *Adv. Technol.*, 2016, 5(1), 53–65.
- F. Brahmi, I. Mateos-Aparicio, K. Mouhoubi, S. Guemouni, T. Sahki, F. Dahmoune, F. Belmehdi, C. Bessai, K. Madani and L. Boulekbache-Makhlouf, *Antioxidants*, 2023, 12, 638.
- F. Brahmi, F. Blando, R. Sellami, S. Mehdi, L. De Bellis, C. Negro, H. Haddadi-Guemghar, K. Madani and L. Makhlouf-Boulekbache, *Ind. Crops Prod.*, 2022, 184, 114977.
- S. Mindjou, F. Brahmi, W. Belkhiri, F. Bouanane, N. Bouchalal and K. Madani, *Curr. Nutr. Food Sci.*, 2020, 16, 190–197.
- F. Brahmi, A. Oufighou, L. Smail-Benazzouz, N. Hammiche, L. Hassaine, L. Boulekbache-Makhlouf, K. Madani and F. Blando, *Resources*, 2024, 13, 124.
- F. Brahmi, D. Hauchar, N. Guendouze, M. Khodir, M. Kiendrebeogo, L. Kamagaj, C. Stévigny, M. Chibane and P. Duez, *Ind. Crops Prod.*, 2015, 74, 722–730.
- M. E. Ala n, M. Ivanović, A. M. G mez-Caravaca, D. Arr ez-Rom n and A. Segura-Carretero, *Arabian J. Chem.*, 2020, 13, 1685–1701.
- O. Kaltsa, S. Grigorakis, A. Lakka, E. Bozinou, S. Lalas and D. P. Makris, *AgriEngineering*, 2020, 2, 226–239.
- D. Chakroun, S. Grigorakis, S. Loupassaki and D. P. Makris, *Biomass Convers. Biorefin.*, 2021, 11, 1125–1136.
- P. V. de Almeida Pontes, I. A. Shiwaku, G. J. Maximo and E. A. C. Batista, *Food Chem.*, 2021, 352, 129346.
- A. E.  nli, *Waste and Biomass Valorization*, 2021, 12, 5329–5346.
- E. Boli, N. Prinos, V. Louli, G. Pappa, H. Stamatis, K. Magoulas and E. Voutsas, *Separations*, 2022, 9, 255.
- H. Akli, S. Grigorakis, A. Kellil, S. Loupassaki, D. P. Makris, A. Calokerinos, A. Mati and N. Lydakis-Simantiris, *Appl. Sci.*, 2022, 12, 831.



- 35 V. Athanasiadis, D. Palaiogiannis, K. Poulianiti, E. Bozinou, S. I. Lalas and D. P. Makris, *Sustainability*, 2022, **14**(11), 6864.
- 36 A. Houasni, S. Grigorakis, A. Kellil and D. P. Makris, *Biomass*, 2022, **2**(1), 46–61.
- 37 M. Alrugaibah, Y. Yagiz and L. Gu, *Food Bioprod. Process.*, 2023, **138**, 198–208.
- 38 P. Siamandoura and C. Tzia, *Molecules*, 2023, **28**(1), 353.
- 39 A. Mir-Cerdà, M. Granados, J. Saurina and S. Sentellas, *Antioxidants*, 2023, **12**, 995.
- 40 A. Mir-Cerdà, M. Granados, J. Saurina and S. Sentellas, *Food Chem.*, 2024, **456**, 140042.
- 41 P. Tapia-Quirós, A. Mir-Cerdà, M. Granados, S. Sentellas and J. Saurina, *Antioxidants*, 2025, **14**(2), 136.
- 42 J. Cubero-Cardoso, M. Hernández-Escaño, A. Trujillo-Reyes, F. G. Feroso, M. A. Fernández-Recamales, J. Fernandez-Bolanos, *et al.*, *Sustainable Chem. Pharm.*, 2025, **43**, 101879.
- 43 D. Bleus, R. B. Jolivet, W. Marchal, D. Vandamme and K. Dziubinska-Kuehn, *J. Mol. Liq.*, 2025, **435**, 128147.
- 44 I. Ahmad, B. D. Hikmawan, L. Febrina, J. Junaidin, A. Rusman, S. Salam, *et al.*, *J. Appl. Pharm. Sci.*, 2025, **15**(11), 089–097.
- 45 R. Rodríguez-Fernández, Á. Fernández-Gómez, J. C. Mejuto and G. Astray, *Foods*, 2023, **12**(24), 4483.
- 46 A. Altop, İ. Coşkun, G. Filik, A. Küçükgül, Y. Genç Bekiroğlu, H. Çayan, E. Güngör, A. Şahin and G. Erener, *Cienc. Invest. Agrar.*, 2018, **45**, 220–230.
- 47 F. Brahmi, B. Mechri, M. Dhibi and M. Hammami, *Ind. Crops Prod.*, 2013, **49**, 256–264.
- 48 I. Khelouf, I. J. Karoui, A. Lakoud, M. Hammami and M. Abderrabba, *Heliyon*, 2023, **9**, e22217.
- 49 F. Abdellah, *Innovations Biol. Sci.*, 2024, **6**, 89–109.
- 50 B. Martín-García, S. De Montijo-Prieto, M. Jiménez-Valera, A. Carrasco-Pancorbo, A. Ruiz-Bravo, V. Verardo and A. M. Gómez-Caravaca, *Antioxidants*, 2022, **11**, 558.
- 51 V. G. Kontogianni and I. P. Gerothanassis, *Nat. Prod. Res.*, 2012, **26**, 186–189.

